Pure & Appl. Chem., Vol. 56, No. 10, pp 1429-1437, 1984.
Printed in Great Britain.

0033-4545/84 $3.00+0.00
Pergamon Press Ltd.

SURFACE ENHANCED RAMAN SCATTERING (SERS) OF MACROMOLECULES ON COLLOIDAL SILVER

Milton Kerker

Department of Chemistry, Clarkson University, Potsdam, NY 13676

Abstract - The remarkable enhancement of Raman signals from molecules on roughened silver surfaces or on silver colloids has made it possible to obtain vibrational spectra with only monolayer and submonolayer coverage. This communication discusses the physical notions underlying this phenomenon and then surveys the as yet limited applications to macromolecules.

INTRODUCTION

The realization that Raman signals from pyridine adsorbed at roughened silver electrodes (Ref. 1) are enhanced 10^5 to 10^6 over signals from dissolved pyridine (Refs. 2,3) unleashed a torrent of investigations that has hardly abated (Refs. 4,5). Suitable substrates for adsorbed molecular species, in addition to the roughened electrodes on which this remarkable phenomenon was first observed, include colloidal metal particles, vacuum-deposited metal island films, matrix isolated metal clusters, roughened surfaces of single crystals under ultra high vacuum, tunnel junction structures, smooth metal surfaces in the attenuated total reflection arrangement, metal-capped polymer posts, and holographic gratings. The initial observations of SERS for adsorbates on gold, silver and copper have been extended to include aluminum, cadmium, lithium, nickel, palladium, platinum and sodium.

Speculations to account for this surface enhanced Raman scattering (SERS) immediately fell into two major categories. A purely physical mechanism was proposed in which the molecules were presumed to respond to gigantic electromagnetic fields generated locally by collective oscillations of the free electrons in small metal structures. In addition, so-called "chemical" mechanisms envisioned charge transfer between metal and adsorbate or else formation of a molecule-metal atom complex with consequent molecular resonances. Such specific molecular interactions may certainly play a role since different molecules on the same surface or different Raman bands of the same molecule may exhibit different SERS effects. Indeed, contributions to SERS from each of these two kinds of mechanisms, electromagnetic and chemical, are not mutually exclusive, yet the preponderant current view is that the major contribution is due to the local field enhancement associated with resonant excitation of electron oscillations, otherwise termed surface plasmons.

Although the vast majority of experimental studies have utilized other substrates, colloidal particles are uniquely advantageous for theoretical analysis. Colloid optics is a venerable subject and we have expanded upon classical light scattering theory in order to articulate a complete electromagnetic field theory of SERS. Not only does this predict the magnitude of the enhancement in agreement with measurements, but it also depicts the remarkable wavelength dependence of SERS upon the optical properties and the morphology of the colloidal particles. The model can be considered as prototypic of the other substrates for none of which has it been possible to derive a definitive theory. Indeed, a substrate such as a "roughened" surface cannot even be described deterministically even though it can be very crudely envisaged as comparable to a smooth surface covered with "colloidal bumps".

The main effort by investigators heretofore has been to elucidate the phenomenon itself rather than to utilize SERS to solve chemical problems. For that reason most studies have focussed upon a relatively small number of molecules and investigations of macromolecules have not been prominent. Yet SERS does open up the possibility of obtaining vibrational spectra of macromolecules in environments hitherto inaccessible. Later in this report we illustrate that

fact by surveying the principal studies which have utilized macromolecules. But first the theory will be outlined only in sufficient detail to enable the reader to grasp the main physical ideas.

ELASTIC SCATTERING BY SMALL PARTICLES

Figure 1 will be utilized in this and the following sections. We first consider elastic scattering, for which the scattered radiation has the same frequency as the incident beam. The particle, which is characterized by its morphology (meaning size, shape and orientation) and its complex refractive index m_o or dielectric constant ε_o ($\varepsilon_o=m_o^2$) relative to the corresponding quantity in the external medium, is irradiated by a plane electromagnetic wave at some angular frequency ω_o ($\omega_o=2\pi\nu_o$). The wave penetrates the particle where this internal field is described by the electric vector $\vec{E}_i(\omega_o,\vec{r}_<)$. For simplicity we omit mention throughout this paper of the corresponding magnetic vector. The field outside of the particle, which is constructed by superposition of the incident field $\vec{E}_o(\omega_o)$ plus a scattered field $\vec{E}_s(\omega_o,\vec{r}_>)$, must be matched at the particle surface with the internal field. Positions inside and outside the particle have been indicated by $\vec{r}_<$ and $\vec{r}_>$ to emphasize that the fields vary strongly with position. The solution of this boundary value problem, which depends upon particle morphology and refractive index, completely characterizes both the scattered electromagnetic fields and the electromagnetic fields inside the particle (Ref. 6).

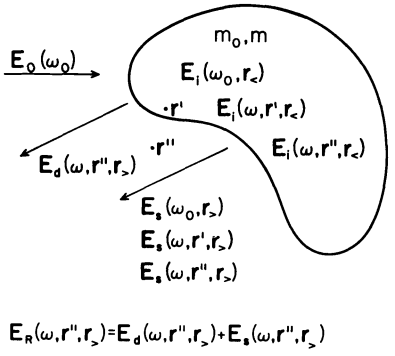

Fig. 1 Model for elastic scattering, inelastic scattering for molecule embedded at $\vec{r}'$, and inelastic scattering for molecule at $\vec{r}''$.

INELASTIC SCATTERING BY EMBEDDED MOLECULES

Now we turn to inelastic scattering, of which fluorescence and the Raman effect are examples. The molecule is treated as a polarizable electric dipole which is excited at one frequency and reemits at some shifted frequency.

There are several important experimental areas of investigation where inelastically scattering molecules are embedded within small particles of which the most active are flow fluorimetry of biological cells and chromosomes, and Raman microprobe analysis of colloids. A number of years ago we raised the following query regarding these experiments: How are inelastic signals affected by embedment of active molecules within small particles? The result has been to show that such signals do indeed depend upon the particle morphology, the refractive index of the particle and the spatial distribution of the active molecules within the particle.

Again we turn to Fig. 1. An inelastically scattering molecule, located at some position $\vec{r}'$ within the particle, is excited by the radiation field at the incident frequency inside the particle and it will radiate at the shifted frequency, ω. The refractive index and dielectric constant at this frequency are m and ε, respectively. The emission dipole moment is equal to the incident internal field (Ref. 7) at location $\vec{r}'$ multiplied by a polarizability tensor $\overset{\leftrightarrow}{\alpha}$ which we will treat as a phenomenological parameter, i.e. $\vec{p}(\omega,\vec{r}') = \overset{\leftrightarrow}{\alpha}\cdot\vec{E}_i(\omega_o,\vec{r}')$. We assume that the polarizability of the molecular dipole is the same as if it were embedded in the bulk medium of which the particle is composed.

The field $\vec{E}_i(\omega,\vec{r}',\vec{r}_<)$ at the shifted frequency ω and arbitrary position $\vec{r}_<$ inside the particle is due to the dipolar emission by the molecule at $\vec{r}'$ and internal reflections from the particle boundary. Analysis of this field and

the scattered field $\vec{E}_s(\omega,\vec{r}',\vec{r}_>)$ leads to a new boundary value problem whose solution completely describes the radiation. Since $\vec{E}_s(\omega,\vec{r}',\vec{r}_>)$ is the solution for only a single molecule located at position $\vec{r}'$, it is necessary, for an array of molecules, to add the results appropriately (coherently or incoherently) to correspond to the particular distribution of material within the particle.

We have formulated the theory and carried out numerical calculations for spheres (Refs. 8-11), concentric spheres (Ref. 12), cylinders (Ref. 13), and spheroids (Refs. 14,15). Some of the main predictions of the theory have been verified by experiments with fluorescent polymer latexes (Refs. 16-21).

MODEL FOR SERS

The path has been straightforward, at least conceptionally, from the theory of elastic scattering by small particles to the above model of inelastic scattering by molecules embedded within small particles. Extension to the case where the active molecules are outside of the particle, including positions at the outer surface, will now be considered.

This model too is depicted in Fig. 1. The molecule, which once again is presumed to behave as an electric dipole, is located at $\vec{r}''$ now taken outside of the particle. The electric field outside the particle at frequency ω_o is comprised of the field of the incident plane wave $\vec{E}_o(\omega_o)$ plus the scattered field $\vec{E}_s(\omega_o,\vec{r}_>)$. This field excites the dipole located at $\vec{r}''$ to radiate at the Raman frequency with induced dipole moment $\vec{p}(\omega,\vec{r}'') = \overleftrightarrow{\alpha}'\cdot[\vec{E}_o(\omega_o,\vec{r}'') + \vec{E}_s(\omega_o,\vec{r}'')]$ where $\overleftrightarrow{\alpha}'$ is the appropriate Raman polarizability tensor. The Raman radiation field in the space outside of the particle including the observer position may now be constructed of two terms, viz. $\vec{E}_R(\omega,\vec{r}'',\vec{r}_>)=\vec{E}_{dip}(\omega,\vec{r}'',\vec{r}_>)+\vec{E}_s(\omega,\vec{r}'',\vec{r}_>)$. The first term is the field that dipole $\vec{p}(\omega,\vec{r}'')$ would exert in the absence of the particle; the second term is an induced or scattered field due to the presence of the particle. The latter may be obtained from solution of the boundary value problem posed by a radiating dipole in the presence of a particle (Ref. 22) which in turn follows from matching $\vec{E}_R(\omega,\vec{r}'',a)$ with the field inside the particle $\vec{E}_i(\omega,\vec{r}'',a)$ at the spherical surface (r=a).

The enhancement is obtained by comparison of the Raman signal in the presence of the particle with that from a molecular dipole having the same polarizability as the surface enhanced dipole but in the absence of the particle, i.e., when the dipole moment is $\vec{p}'(\omega,\vec{r}'') = \overleftrightarrow{\alpha}'\cdot\vec{E}_o(\omega_o,\vec{r}'')$. If the field due to this dipole is $\vec{E}_d'(\omega,\vec{r}'',\vec{r}_>)$, the enhancement becomes $G=|\vec{E}_R(\omega,\vec{r}'',\vec{r}_>)|^2/|\vec{E}_d'(\omega,\vec{r}'',\vec{r}_>)|^2$.

It is also necessary to consider the orientation of the various dipoles. In practice, our calculations have been performed by comparing Raman signals from a particle uniformly covered by dipoles whose axes are normal to the surface with a similar arrangement of oriented dipoles in the solution. We assume that the absorption and emission dipoles are similarly oriented but uncorrelated in phase. In the case of spheroids, the particles are also taken to be randomly oriented.

Obviously, the Raman polarizability of the molecular dipole may be altered upon adsorption, but if known from either experiment or theoretical analysis, that information can be incorporated into the model by providing the appropriate value of $\overleftrightarrow{\alpha}'$. Thus while this electromagnetic model provides the necessary framework for the model, it can be enriched by any specific chemical information should that be available.

We have been able up to now to obtain a completely general solution only for homogeneous spheres and the numerical results for that case will be presented in the next section. Following that, we will consider solutions for spheroids and concentric spheres subject to the limitation that the particles be small compared to the wavelengths.

Spheres

The mathematical analysis and more detailed calculations for homogeneous spheres are given elsewhere (Refs. 23,24). The model describes the dependence of the angular distribution and polarization of the SERS upon the size and dielectric properties of the particle as well as on the orientation of the molecular dipoles and their distance from the surface. The sampling of numerical results presented here is intended merely to illustrate some the main physical features of the phenomenon. The optical constants of silver (Ref. 25) are used because they exhibit the most striking effects. Indeed, that is

why silver has been used in most of the experimental work. It should be borne in mind that values of these constants obtained from measurements on bulk samples may not be valid for small particles because of quantum size effects (Ref. 26) and also because there may be specific phase and structural effects within any particular preparation of small particles which differ from the bulk. Although incorporation of such perturbations affects the quantitative aspects of computed results, the main qualitative features are not changed (Ref. 24). The Raman shift has been selected in most cases illustrated here at 1010 cm^{-1} to correspond to this much studied pyridine line. The upper value of particle radius a = 500 nm has been dictated by the computational time requirements rather than by any limitations of the theoretical analysis. The larger the particle size, the more lengthy the calculation.

Figure 2 depicts the enhancement as a function of excitation wavelength, the excitation profile, for a monolayer at the surface of 5, 50 and 500 nm radius silver spheres immersed in water. The magnitude of the doubly-peaked maximum for the 5 nm particle corresponds in value to the largest experimental measurements (10^5 to 10^6). For a = 50 nm, the enhancement maximum of 10^4 is much broader and is shifted to longer wavelengths. For the still larger particle, a = 500 nm, the enhancement oscillates in the 10 to 10^2 range through the visible.

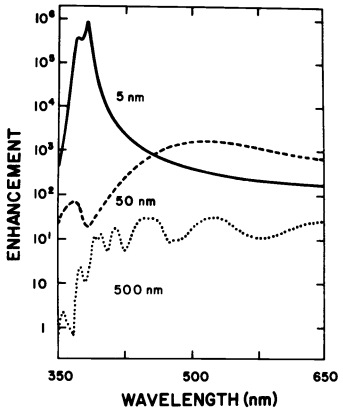

Fig. 2 Excitation profile for enhancement of 1010 cm^{-1} Raman band for a monolayer adsorbed on 5, 50 and 500 nm radius Ag sphere in water.

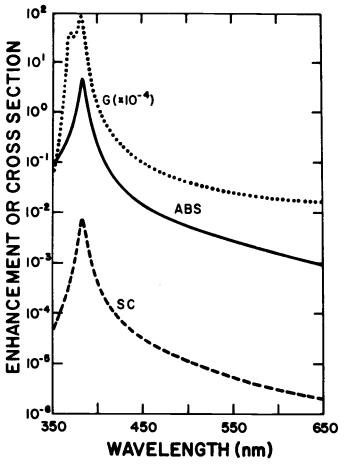

Fig. 3 Comparison of excitation profile of 5 nm radius Ag sphere in water with absorption and scattering spectra.

The peak value of 10^6 occurs only at about 382 nm and only for particles with radii about 10 nm and smaller. The origin of this huge enhancement can be envisaged if we consider a very much simplified expression for the enhancement in the limiting case that the particle be very much smaller than the wavelength, viz.

$$G = |(1+2g)(1+2g_o)|^2 \tag{1}$$

where

$$g = \frac{\varepsilon-1}{\varepsilon+2} = \frac{m^2-1}{m^2+2}; \quad g_o = \frac{\varepsilon_o-1}{\varepsilon_o+2} = \frac{m_o^2-1}{m_o^2+2} . \tag{2}$$

When much smaller than the wavelength, the particle behaves as if it were a polarizable dipole with polarizability a^3g. In a formal sense excitation of the dipole surface plasmon, which results in SERS, takes place whenever there is a resonance as the denominators of g and g_o become small as a consequence of ε_o and ε, approaching the value -2. This occurs for silver in water at about 382 nm. Actually, these expressions do not blow up, even where $\varepsilon = -2$, because higher order terms contribute to both numerator and denominator of g, g_o as $\varepsilon+2$ becomes small (Refs. 23,24).

The physical origin of the resonance can be understood in terms of the Drude model (Ref. 27). When the free electrons oscillate in phase with the electromagnetic field the dielectric constant become a real negative number (the refractive index becomes a purely imaginary number). A small particle, now conceived of as a cavity of oscillating free electrons, will have a characteristic frequency at which it will resonate. For very small spheres this so-called dipolar surface plasmon is excited to resonance whenever $\varepsilon = -2(m=\sqrt{2}i)$.

The enhanced electric fields associated with excitation of the dipolar surface plasmon also results in enhanced absorption and scattering as shown in Fig. 3 where the SERS excitation profile, the absorption spectrum and the scattering spectrum of a 5 nm radius silver sphere in water are compared (Ref. 28). Note how each of these peak at precisely the same excitation wavelength.

For larger spheres there will, in addition to the dipolar mode, be a hierarchy of higher order modes all of which contribute to the various optical processes associated with the spherical particles. Any one of these may be resonantly excited at a particular frequency which depends upon particle size and optical constants. However, unlike a small particle where only the dipolar mode is active, in a larger particle there are a large number of contributing modes so that resonant excitation of one of these will have a smaller effect on the total process. Furthermore, the partial electric fields associated with these higher modes will have a different spatial distribution inside the particle from that near the outer particle surface. Thus resonant excitation of particular modes may result in very strong fields localized at radial positions inside the particle somewhat removed from the particle surface, thereby giving rise to strong absorption (Ref. 29). Resonant excitation of other modes may give rise to strong fields localized just outside the particle surface, giving rise to SERS. Accordingly the absorption and scattering spectra which arise from excitation of the lossy dipoles composing the particle will be decoupled from the SERS excitation spectrum which depends upon the local fields outside of the particle. It should be emphasized, therefore, that the absorption and scattering spectra are coupled with the SERS excitation profile only when the particles are sufficiently small to be treated in the dipole limit.

Spheroids

The most striking feature of SERS is that the gigantic enhancement occurs over a narrow wavelength region and that for spheres much smaller than the wavelength this excitation profile parallels a sharp band in the absorption and scattering spectra (Fig. 3). These effects have been attributed physically to enhanced electric fields due to resonant excitation of the conduction electrons. Formally, they occur whenever the expression for the polarizability factor of the particle (Eq. 2) becomes large due to its denominator becoming small.

The treatment in this section will be restricted to the small particle limit. The polarizability along any particular semi-axis of an ellipsoidal particle very much smaller than the wavelength is $(abc)g_i$ where

$$g_i = \frac{\varepsilon-1}{3[1+(\varepsilon-1)P_i]}, \quad i = a,b,c \tag{3}$$

and the depolarization factor P_i depends upon the values of the three semi-axes of the ellipsoid, a,b,c (Ref. 6). For a sphere the triply degenerate values of $P_i = 1/3$ so that resonance, as we have already seen, occurs whenever $\varepsilon = -2$. For an ellipsoid there may be three distinct absorption bands corresponding to the three values of P_i; for a spheroid there may be two bands, one of which will be doubly degenerate.

This has long been a known feature of the optical absorption of small particles and Fig. 4 illustrates the change of the absorption spectrum of small silver particles in water as the shape of the equivolume particles varies from spherical to increasingly elongated prolate spheroids (Ref. 28). The triply degenerate absorption band at 382 nm for the sphere splits into two bands, which depend upon the two semi-axes of the spheroid, one of these at a lower wavelength and a doubly degenerate one at a higher wavelength. For a 3 to 1 axial ratio, the longer wavelength band has shifted to 580 nm. In the parlance of the resonance model, there is a dipolar surface plasmon resonating at each of these wavelengths.

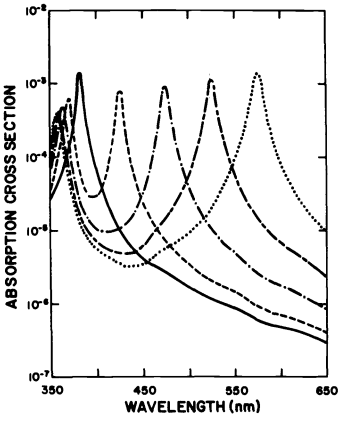

Fig. 4 Absorption spectra for small Ag sphere in water (——) and prolate spheroids with axial ratios 1.5, 2.0, 2.5, 3.0 (left to right).

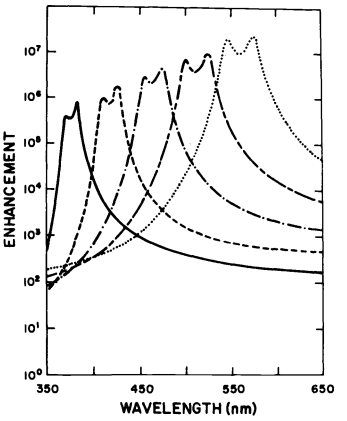

Fig. 5 Excitation profile for 5 nm radius Ag sphere in water (——) and prolate spheroids with axial ratios 1.5, 2.0, 2.5, 3.0 (left to right).

It is not surprising that there is a similar effect upon the SERS excitation profile. We have utilized the same physical model as for spheres but because of the added mathematical complexities have only obtained a result valid for particles which are small relative to the wavelength (Ref. 28). Somewhat similar results were also obtained by Gersten and Nitzan (Ref. 30) and by Adrian (Ref. 31). A typical calculation is shown in Fig. 5 where the excitation profile for a silver particle in aqueous medium is plotted as a sphere is deformed into an increasingly elongated equivolume spheroid. The molecular dipoles are assumed to form a monolayer and to be oriented normal to the surface, and the particles are assumed to be randomly oriented. Not only does the strongly enhanced band shift but the enhancement itself increases by an order of magnitude. The longer wavelength branch of the bimodal peak occurs in each instance at the same wavelength as the peak in the corresponding absorption spectrum (see Fig. 5) and the separation of the two modes in the SERS band equals the Raman shift, in this instance 1010 cm^{-1}.

Concentric spheres

1. Active molecules located outside of concentric spheres. In this case a particle of radius b is comprised of two regions, a spherical core of radius a and an outer concentric spherical shell. The Raman active molecules are taken to be outside the sphere. Only the limiting case that the particle be small compared to the wavelength is treated so that the enhancement is given by Eq. (1) where the polarizability factor of the particle is

$$g = \frac{(\varepsilon_2-1)(\varepsilon_1+2\varepsilon_2) + q^3(2\varepsilon_2+1)(\varepsilon_1-\varepsilon_2)}{(\varepsilon_2+2)(\varepsilon_1+2\varepsilon_2) + q^3(2\varepsilon_2-2)(\varepsilon_1-\varepsilon_2)} \tag{4}$$

and ε_1 and ε_2 are the dielectric constants of the core and spherical shell regions relative to the medium and q = b/a (Ref. 6,32). There is a similar expression for g_o.

There are now two possibilities for exciting strong resonances, either when the spherical shell is composed of a plasma such as silver and the core is a dielectric material or the reverse situation when the core is composed of a plasma. Some SERS excitation profiles (Ref. 33) are illustrated in Fig. 6 for the former case. The dependence of the SERS excitation profile upon the particular morphology is once again apparent. Furthermore, it depends not only upon the dielectric constant of the metallic region, but also upon that of the dielectric regions within the particle and of the external medium. In this case the external medium has been taken as air rather than water. This increases the relative dielectric constant of silver by the factor 1.77 which has the effect of lowering the enhancement substantially. There are somewhat similar effects when the plasma is at the core of the particle.

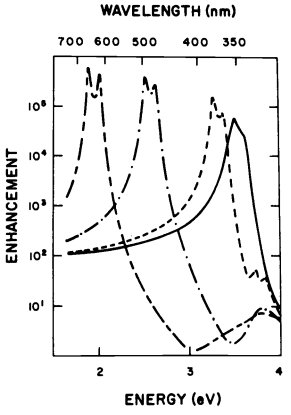

Fig. 6 Excitation profile for 5 nm radius silver coated dielectric (m = 1.5) sphere in air with ratio of dielectric core radius to total radius 0, 0.5, 0.8 and 0.9 (from right to left).

2. Active molecules located within spherical shell. In this case the active molecules are treated as electric dipoles embedded within the dielectric spherical shell which coats the metallic core, rather than as a monolayer dangling out in the medium external to the particle. The field within the dielectric shell at the incident frequency which stimulates the Raman dipole must first be calculated and the boundary value problem posed by a dipole radiating from within the dielectric shell must be solved. The full analysis had been treated earlier (Ref. 12) but the complexity of the resulting expressions had precluded numerical computation. The limiting case of a particle which is small compared to the wavelength requires solution only of the electrostatic problem and elucidation of this limiting case (Ref. 34) has avoided lengthy programming and computation.

It has been possible to locate conditions for which the resonance condition can be strongly affected by the dielectric layer. In such a case, corresponding to a metal particle coated with such a dielectric layer, perhaps an oxide, in which Raman active molecules are entrapped, the SERS excitation profile may be shifted and the peak enhancement itself may be sharply affected (Ref. 35).

SERS EXPERIMENTS WITH MACROMOLECULES

We initiate our survey by considering the work of Murray et al (Ref. 36,37) who have explored the question of whether SERS requires direct contact with the metal by interspersing a weakly Raman scattering polymer, poly(methylmethacrylate) PMMA between a strongly Raman active polymer poly(p-nitrostyrene) PPNS and a roughened silver surface. These authors had the capability, using a spin-casting technique, of varying the thickness of each layer. They observed an enhancement of about 10^6 for direct contact of PPNS with a fall off of the enhancement of about 10 with each 35-50 Å thickness layer of PPNS. This was consistent with the electromagnetic field model since it demonstrated that SERS did not require molecular contact with the metal surface. Furthermore, it makes possible the use of these large local fields to probe the vibrational structure of polymers very close to the surface.

Although infrared and Raman spectroscopy have been used to characterize the vibrational structure of polymers their application to surface analysis has been limited mainly to internal reflectance infrared spectroscopy which has the drawback of a large probing depth. Because of this it is difficult to separate vibrational features of the outermost surface from the bulk features arising several micrometers into the surface. However, good quality vibrational spectra of very thin polymer films can be obtained using the SERS effect. Indeed, Allara, Murray and Bodoff (Ref. 38) have noted that by varying the particular metal substrate or the morphology of the surface one can vary the effective penetration depth of the Raman probe from less than 20 Å to about 200 Å. Since the enhancements are of the order of 10^4 to 10^7 compared to the bulk material, the spectrum of the near surface region of a thick sample is greatly magnified compared to the signals from the bulk of the sample.

An example of the application of SERS to study biopolymers adsorbed from solution has been the monitoring of the mediation by 4,4'-bipyridine of the

electron transfer of cytochrome c and a silver electrode (Ref. 39). In the case of biopolymers such as cytochrome c and myoglobulin which are chromophores, when the excitation wavelength coincides with an absorption band, the ensuing resonance Raman spectrum (RR) may be enhanced by several orders of magnitude over spectra obtained outside of the absorption band. If, in addition, the excitation also coincides with the optical resonance of the surface features of the colloidal particles which gives rise to SERS, this coincidence of RR and SERS may be multiplicative leading to enormous enhancements (Ref. 40). This makes possible the detection of extremely small amounts of such biopolymers.

Koglin et al. have reported SERS signals from DNA, poly-A (Ref. 41) and the nucleic acid bases (Ref. 42) on both silver electrode surfaces and colloidal silver. Their group has been using electrochemical techniques to study nucleic acids at the charged mercury-water interface as a model for their behavior at charged biological surfaces. Normal solution scattering of DNA, for example, shows prominent Raman bands which are associated with the nucleic acid bases. These bases themselves exhibit strong SERS signals at the same frequencies when adsorbed on roughened silver electrode surfaces or on silver colloids. On the other hand intact DNA, similarly adsorbed, shows only minor enhancement for nucleic acid bands although there is significant enhancement of bands associated with the sugar-phosphate groups. The interpretation is that the latter, located on the outside of the molecule, are very close to the surface whereas the bases are further removed, being at the center of the helix. Yet when exposed to γ-radiation the nucleic acid bands appear. With increasing radiation there is a striking enhancement of the ring modes of the bases suggesting that these become more accessible to the silver surface. This confirms the well-known fact that ionizing radiation causes damage in DNA consisting of strand breaks which induce labilization of the helical structure. From the point of view of this report it provides a dramatic instance of the utility of SERS as a tool for probing configuration on a surface.

There is an advantage to working with a surface with a well-defined structure rather than so-called roughened surfaces which cannot be readily reproduced and which are not amenable to theoretical analysis. Holographic gratings comprise one such controlled surface and thin polystyrene films deposited on holographic gratings of metallic silver (Ref. 43) and gold (Ref. 44) have given SERS signals. The undulations in presently available gratings however appear to give enhancements only in the range 50 to 80.

Colloidal particles may also serve to provide a controlled surface. In addition, the only definitive theory, that outlined in this report, is applicable to colloids. SERS signals have been observed from polymers adsorbed on these. For example, metal colloids utilized as catalysts in the photochemical splitting of water are frequently stabilized by polymers. Since subtle changes in polymer structure appears to affect the stability and thereby the catalytic activity (Ref. 45), it is clear that SERS could potentially provide structural information to account for such effects. Indeed, SERS has been reported for poly(vinyl alcohol), poly(vinyl pyridine), poly(ethylene glycol) (Ref. 46) and polyvinyl (pyrollidone) (Ref. 47) on gold and silver hydrosols. The degree of enhancement of the various bands in the spectrum made it possible to suggest the manner in which each macromolecule was attached to the surface.

We have prepared a silver organosol in ethanol in which PVPR serves as a protective polymer coating (Ref. 48). SERS spectra exhibited chain vibrations similar to other singly-substituted vinyl polymers. By coadsorbing a chromophoric molecule, dabsyl aspartate, it was possible to delineate separately the effects of normal Raman and resonance Raman scattering on the same surface. The competition of the polymer and the dye for surface sites was studied and the effect of polymer molecular weight in this competition as well as its effect on protection action by the polymer could be elucidated (Ref. 49).

REFERENCES

1. M.J. Fleischmann, P.J. Hendra and A.J. McQuillan, Chem. Phys. Lett. 26, 163-166 (1974).
2. D.J. Jeanmaire and R.P. Van Duyne, J. Electroanal. Chem. 84, 1-20 (1977).
3. M.G. Albrecht and J.A. Creighton, J. Am. Chem. Soc. 99, 5215-5217 (1977).
4. R.K. Chang and T.E. Furtak, Surface Enhanced Raman Scattering, Plenum Press, New York (1982).

5. A. Otto, in Light Scattering in Solids, Vol. IV, eds. M. Carbona and G. Guntherodt, Springer, New York (1983).
6. M. Kerker, The Scattering of Light and other Electromagnetic Radiation, Academic Press, New York (1969).
7. P.W. Dusel, M. Kerker and D.D. Cooke, J. Opt. Soc. Am. 69, 55-59 (1979).
8. H. Chew, P.J. McNulty and M. Kerker, Phys. Rev. A 13, 396-404 (1976).
9. M. Kerker, P.J. McNulty, M. Sculley, H. Chew and D.D. Cooke, J. Opt. Soc. Am. 68, 1676-1686 (1978).
10. H. Chew, M. Sculley, M. Kerker, P.J. McNulty and D.D. Cooke, J. Opt. Soc. Am. 68, 1686-1639 (1978).
11. M. Kerker and S.D. Druger, Appl. Opt. 18, 1172-1179 (1979).
12. H. Chew, M. Kerker and P.J. McNulty, J. Opt. Soc. Am. 66, 440-444 (1976).
13. H. Chew, D.D. Cooke and M. Kerker, Appl. Opt. 19, 44-52 (1980).
14. D.-S. Wang, M. Kerker and H. Chew, Appl. Opt. 19, 2315-2328 (1980).
15. M. Kerker, D.-S. Wang and H. Chew, Cytometry 1, 161-167 (1980).
16. J.P. Kratohvil, M.P. Lee and M. Kerker, Appl. Opt. 17, 1978-1980 (1978).
17. P.J. McNulty, S.D. Druger, M. Kerker and H. Chew, Appl. Opt. 18, 1484-1486 (1979).
18. M. Kerker, M. van Dilla, A. Brunsting, J.P. Kratohvil, P. Hsu and D.-S. Wang, Cytometry 3, 71-78 (1982).
19. E.-H. Lee, R.E. Benner, J.B. Fenn and R.K. Chang, Appl. Opt. 17, 1980-1982 (1978).
20. R.E. Benner, R. Dornhaus, M.B. Long and R.K. Chang, Microbeam Analysis, D.E. Newberry, Ed., San Francisco Press, San Francisco (1979).
21. R.E. Benner, J.F. Owen and R.K. Chang, J. Phys. Chem. 84, 1602-1606 (1980).
22. H. Chew, M. Kerker and D.D. Cooke, Phys. Rev. A 16, 320-323 (1977).
23. D.-S. Wang, H. Chew and M. Kerker, Appl. Opt. 19, 2256-2257 (1980).
24. M. Kerker, D.-S. Wang and H. Chew, Appl. Opt. 19, 4159-4174; this is a rerun of the version published on p. 3373 in which the many typographical errors were not amended.
25. P.B. Johnson and R.W. Christy, Phys. Rev. B 6, 4370-4379 (1972).
26. U. Kreibig and C.V. Fragstein, Z. Phys. 224, 307-323 (1979).
27. C.F. Bohren and D.R. Huffman, Absorption and Scattering of Light by Small Particles, Wiley-Interscience, New York (1983).
28. D.-S. Wang and M. Kerker, Phys. Rev. B 24, 1777-1790 (1981).
29. J.F. Owen, R.K. Chang and P.W. Barber, Opt. Letters 6, 540-542 (1981).
30. J. Gersten and A. Nitzan, J. Chem. Phys. 73, 3023-3037 (1980).
31. F.J. Adrian, Chem. Phys. Lett. 78, 45-49 (1981).
32. A.L. Aden and M. Kerker, J. Appl. Phys. 22, 1242-1246 (1951).
33. M. Kerker and C.G. Blatchford, Phys. Rev. B 26, 4052-4063 (1982).
34. D.-S. Wang and M. Kerker, Phys. Rev. B 25, 2433-2449 (1982).
35. M. Kerker and D.-S. Wang, Chem. Phys. Lett. 104, 516-519 (1984).
36. C.A. Murray and D.L. Allara, J. Chem. Phys. 76, 1290-1303 (1982).
37. C.A. Murray, D.L. Allara, A.F. Hebard and F.J. Padden, Jr., Surface Sci. 119, 449-478 (1982).
38. D.L. Allara, C.A. Murray and S. Bodoff, in Physicochemical Aspects of Polymer Surfaces, Vol. I, Ed. K.L. Mittal, Plenum Press, New York (1983).
39. T.M. Cotton, D. Kaddi and D. Iorga, J. Am. Chem. Soc. 105, 7462-7464 (1983).
40. T.M. Cotton, S.G. Schutz and R.P. Van Duyne, J. Am. Chem. Soc. 102, 7960-7962 (1980).
41. E. Koglin and J.-M. Sequaris, Journal de Physique 44, (C10) 487-490 (1983).
42. E. Koglin, J.-M. Sequaris and P. Valenta, J. Molecular Structure 79, 185-189 (1982).
43. A. Girlando, M.R. Philpott, D. Heitman, J.D. Swalen and R. Santi, J. Chem. Phys. 79, 5187-5191 (1980).
44. M. Metcalfe and R.F. Hester, Chem. Phys. Lett. 94, 411-414 (1983).
45. P.A. Brugger, P. Cundet and M. Gratzel, J. Am. Chem. Soc. 103, 2923-(1981).
46. P.C. Lee and D. Meisel, Chem. Phys. Lett. 99, 262-266 (1983).
47. S.M. Heard, F. Grieser and C.G. Barraclough, Chem. Phys. Lett. 95, 154-158 (1983).
48. O. Siiman, A. Lepp and M. Kerker, Chem. Phys. Lett. 100, 163-168 (1983).
49. A. Lepp and O. Siiman, J. Phys. Chem. Submitted (1984).

Acknowledgment: This work was supported by Army Research Office Grant DAAG-29-82-K-0062 and by National Science Foundation Grant CHE-801144.